

The roles of ATP synthase and the cytochrome *b₆/f* complexes in limiting chloroplast electron transport and determining photosynthetic capacity

Wataru Yamori, Shunichi Takahashi, Amane Makino, Dean Price, Murray Badger and Susanne von Caemmerer

Supplemental Figure Legends

Fig. S1

CO₂ response of CO₂ assimilation rate (*A*) and electron transport rate (ETR) at 25°C. CO₂ response of CO₂ assimilation rate (*A*) measured at 25°C and 1200 μmol photons m⁻² s⁻¹ in anti-ATP synthase (δ) lines (A) or anti-Rieske FeS lines (B). Three groups were classified with respect to ATP synthase (δ) content or Rieske FeS content: Rieske FeS: WT (approximately 100%: circle), plants with intermediate Rieske FeS level (58~85%: triangle) and plants with low Rieske FeS level (27~29%: square); ATP synthase (δ): WT (approximately 100%), plants with intermediate ATP synthase (δ) level (48~75%) and plants with low ATP synthase (δ) level (22~26%). CO₂ assimilation rate at 380 μmol mol⁻¹ CO₂ concentration (*A*₃₈₀) is shown as a solid symbol. CO₂ assimilation rate limited by RuBP carboxylation (*A_c*: solid line) whereas CO₂ assimilation rate limited by RuBP regeneration (*A_r*: dotted line). Curve fitting was described in the material and methods section. CO₂ response of the electron transport rate (ETR) from Chl fluorescence at 25°C at 1200 μmol photons m⁻² s⁻¹ in anti-ATP synthase (δ) lines (C) or anti-Rieske FeS lines (D). ETR at 380 μmol mol⁻¹ CO₂ concentration is shown as a solid symbol. Data represent means ±SE, n = 3~4.

Fig. S2

CO₂ response of CO₂ assimilation rate (*A*) and electron transport rate (ETR) at 40°C. CO₂ response of CO₂ assimilation rate (*A*) measured at 40°C and 1200 μmol photons m⁻² s⁻¹ in anti-ATP synthase (δ) lines (A) or anti-Rieske FeS lines (B). Three groups were classified with respect to ATP synthase (δ) content or Rieske FeS content: wild type (circles), plants with intermediate contents of ATP synthase (δ) or Rieske FeS protein (triangles) and plants with low contents of ATP synthase (δ) or Rieske FeS protein (squares), as mentioned in Fig. S1. CO₂ assimilation rate at 380 μmol mol⁻¹ CO₂ concentration (*A*₃₈₀) is shown as a solid symbol. CO₂ assimilation rate limited by RuBP carboxylation (*A_c*: solid line) whereas CO₂ assimilation rate limited by RuBP regeneration (*A_r*: dotted line). Curve fitting was described in the material and methods section. CO₂ response of the electron transport rate (ETR) from Chl fluorescence at 40°C at 1200 μmol photons m⁻² s⁻¹ in anti-ATP synthase (δ) lines (C) or anti-Rieske FeS lines (D). ETR at 380 μmol mol⁻¹ CO₂ concentration is shown as a solid symbol. Data represent means ±SE, n = 3~4.

Fig. S3

Rubisco activation state, Rubisco and Rubisco activase content. Content of Rubisco (A, B) and Rubisco activase (C, D), and Rubisco activation state (E, F) in antisense plants with a variety of δ subunit of chloroplast ATP synthase (A, C & E) and in antisense plants with a variety of Rieske FeS contents (B, D & F). The contents of several photosynthetic components, including Rubisco and Rubisco activase, were similar among wild type, anti-Rieske FeS plants and anti-ATP synthase (δ) plants. The optimum temperature for A_{380} was $32.3 \pm 0.4^\circ\text{C}$ in WT and was similar among WT, anti-Rieske FeS and anti-ATP synthase (δ). Rubisco activation state at 40°C decreased by 7~8% compared to 25°C in WT. Rubisco activation state declined only by approximately 10% at both 25 and 40°C in anti-ATP synthase (δ) plants with an ATP synthase (δ) content of less than 20% of wild-type. On the other hand, Rubisco activation state declined by approximately 20% both at 25 and 40°C in plants with Rieske FeS content lower than 20% of wild-type

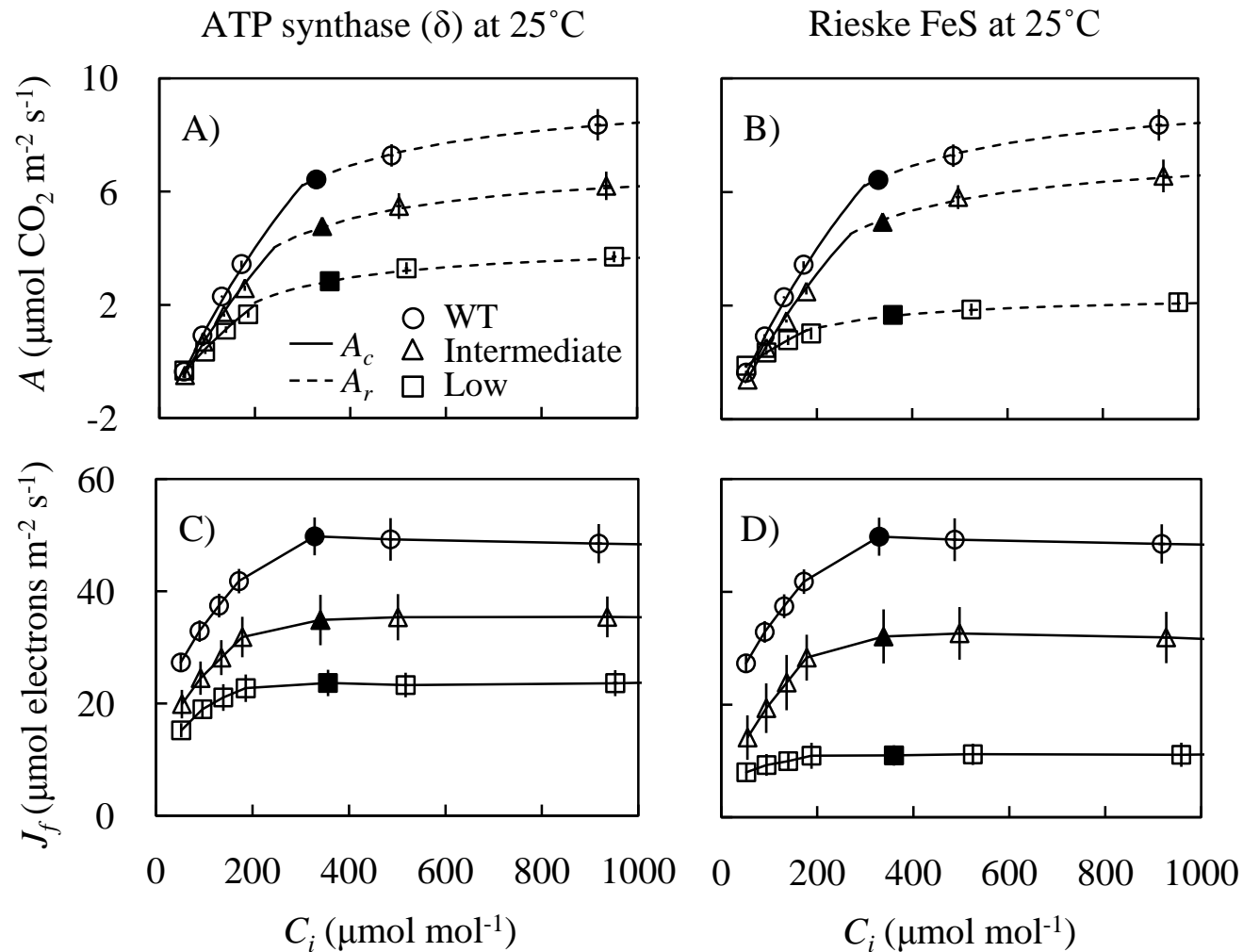


Fig. S1

CO₂ response of CO₂ assimilation rate (A) and electron transport rate (ETR) at 25°C. CO₂ response of CO₂ assimilation rate (A) measured at 25°C and 1200 $\mu\text{mol photons m}^{-2} \text{ s}^{-1}$ in anti-ATP synthase (δ) lines (A) or anti-Rieske FeS lines (B). Three groups were classified with respect to ATP synthase (δ) content or Rieske FeS content: Rieske FeS: WT (approximately 100%: circle), plants with intermediate Rieske FeS level (58~85%: triangle) and plants with low Rieske FeS level (27~29%: square); ATP synthase (δ): WT (approximately 100%), plants with intermediate ATP synthase (δ) level (48~75%) and plants with low ATP synthase (δ) level (22~26%). CO₂ assimilation rate at 380 $\mu\text{mol mol}^{-1}$ CO₂ concentration (A_{380}) is shown as a solid symbol. CO₂ assimilation rate limited by RuBP carboxylation (A_c : solid line) whereas CO₂ assimilation rate limited by RuBP regeneration (A_r : dotted line). Curve fitting was described in the material and methods section. CO₂ response of the electron transport rate (ETR) from Chl fluorescence at 25°C at 1200 $\mu\text{mol photons m}^{-2} \text{ s}^{-1}$ in anti-ATP synthase (δ) lines (C) or anti-Rieske FeS lines (D). ETR at 380 $\mu\text{mol mol}^{-1}$ CO₂ concentration is shown as a solid symbol. Data represent means \pm SE, $n = 3\sim 4$.

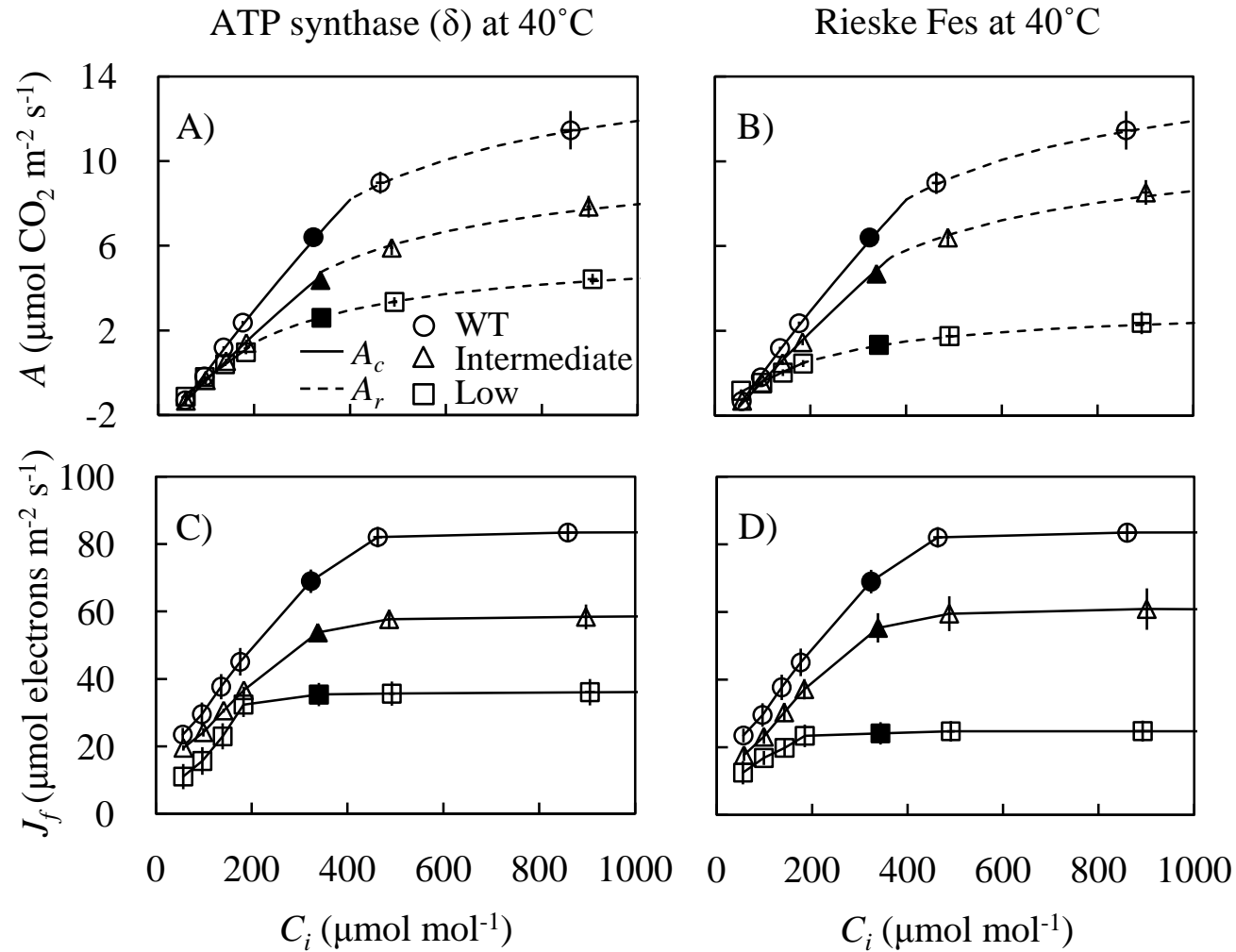


Fig. S2

CO₂ response of CO₂ assimilation rate (A) and electron transport rate (ETR) at 40°C. CO₂ response of CO₂ assimilation rate (A) measured at 40°C and 1200 $\mu\text{mol photons m}^{-2} \text{ s}^{-1}$ in anti-ATP synthase (δ) lines (A) or anti-Rieske FeS lines (B). Three groups were classified with respect to ATP synthase (δ) content or Rieske FeS content: wild type (circles), plants with intermediate contents of ATP synthase (δ) or Rieske FeS protein (triangles) and plants with low contents of ATP synthase (δ) or Rieske FeS protein (squares), as mentioned in Fig. S1. CO₂ assimilation rate at 380 $\mu\text{mol mol}^{-1}$ CO₂ concentration (A_{380}) is shown as a solid symbol. CO₂ assimilation rate limited by RuBP carboxylation (A_c : solid line) was whereas CO₂ assimilation rate limited by RuBP regeneration (A_r : dotted line). Curve fitting was described in the material and methods section. CO₂ response of the electron transport rate (ETR) from Chl fluorescence at 40°C at 1200 $\mu\text{mol photons m}^{-2} \text{ s}^{-1}$ in anti-ATP synthase (δ) lines (C) or anti-Rieske FeS lines (D). ETR at 380 $\mu\text{mol mol}^{-1}$ CO₂ concentration is shown as a solid symbol. Data represent means \pm SE. $n = 3\sim 4$.

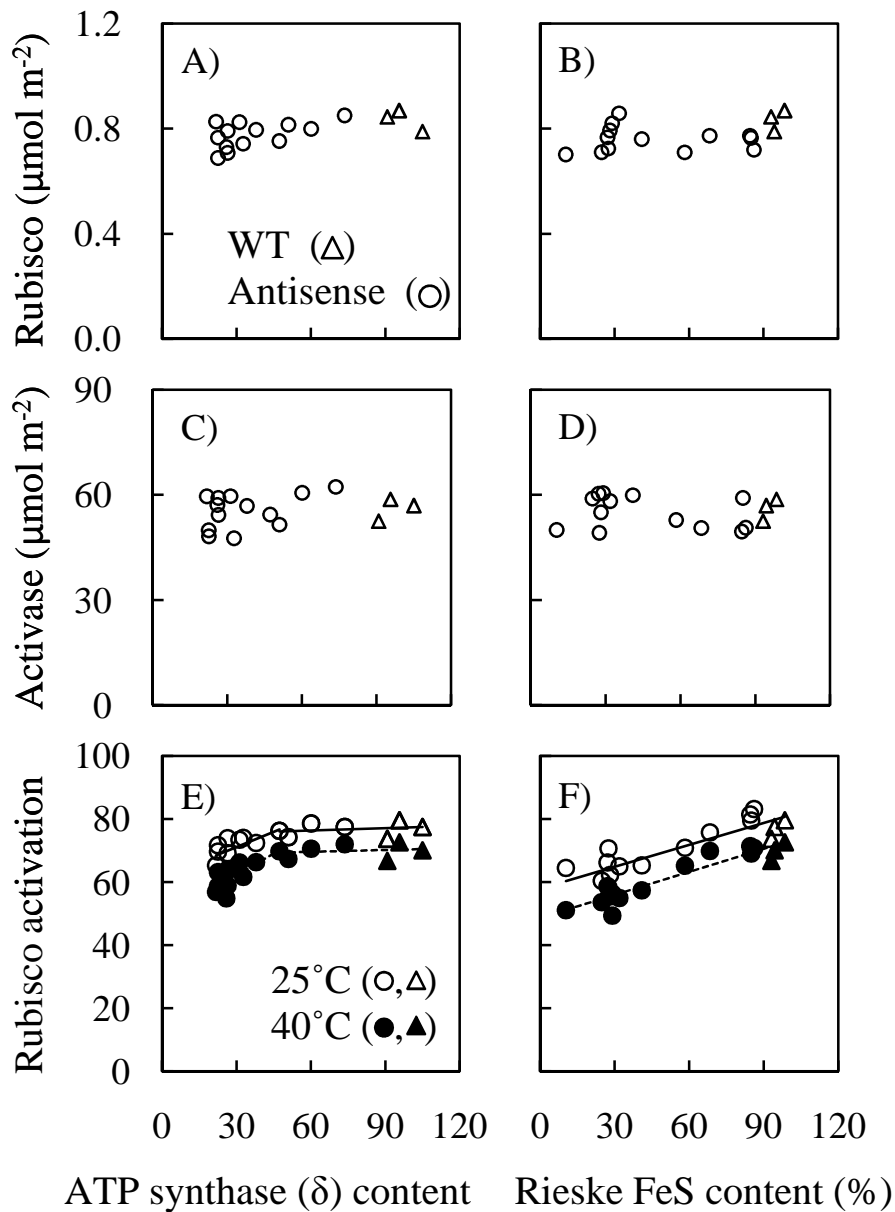


Fig. S3

Rubisco activation state, Rubisco and Rubisco activase content. Content of Rubisco (A, B) and Rubisco activase (C, D), and Rubisco activation state (E, F) in antisense plants with a variety of δ subunit of chloroplast ATP synthase (A, C & E) and in antisense plants with a variety of Rieke FeS contents (B, D & F). The contents of several photosynthetic components, including Rubisco and Rubisco activase, were similar among wild type, anti-Rieske FeS plants and anti-ATP synthase (δ) plants. The optimum temperature for A_{380} was $32.3 \pm 0.4^\circ\text{C}$ in WT and was similar among WT, anti-Rieske FeS and anti-ATP synthase (δ). Rubisco activation state at 40°C decreased by 7~8% compared to 25°C in WT. Rubisco activation state declined only by approximately 10% at both 25 and 40°C in anti-ATP synthase (δ) plants with an ATP synthase (δ) content of less than 20% of wild-type. On the other hand, Rubisco activation state declined by approximately 20% both at 25 and 40°C in plants with Rieske FeS content lower than 20% of wild-type.